International Journal of Mechanical and Production Engineering Research and Development (IJMPERD)
ISSN (P): 2249–6890; ISSN (E): 2249–8001
Vol. 11, Issue 6, Dec 2021, 147–164

Original Article

DEVELOPMENT AND COMPARATIVE EVALUATION OF CONTROLLED WATER JET IMPINGEMENT COOLING SYSTEM FOR HOT-ROLLED STEEL PLATES BY MECHANICAL AND METALLURGICAL ASSESSMENTS

DR. ONAH T. O[1].*, DR. EDEH, J. C[2] & DR. NWANKWOJIKE, B. N[3]

*[1]*Department of Mechanical and Production Engineering, Enugu State University of Science and Technology Enugu, Enugu Nigeria*

[2,3]*Department of Mechanical Engineering, Michael Okpara University of Agriculture, Umudike, Nigeria*

ABSTRACT

Design and development of Water Jet Impingement Cooling System for improving mechanical and metallurgical properties of steel using locally sourced materials was carried out. The modification comprised the introduction of water pump, adjustable impingement gap mechanism and replacement of complicated hydraulic/chain conveyor mechanism with screw conveyor mechanism. The plant was designed, fabricated and instrumented with temperature and flow probes to simulate the actual operating conditions of the steel mill industry. Comparative performance results revealed an 8% increase in the cooling rate of the improved system over the existing technology. Results further showed that with a test-plate initial temperature at 550oC, a controlled cooling temperature of 160oC was achieved which produced film and nucleate boiling heat extraction effect. This influenced the microstructural properties of the test plates. The plates post treatment examinations of the grain microstructure and mechanical properties revealed good martensite-phase transformation and enhanced "advanced-steel" hardness of Rockwell 59.9 respectively. In addition, the impact energy test showed a good value range of 56 to 63J which compared favorably with AISI standard of 44.3J. This, therefore, gave 53% hardness and 26% to 42.2% impact of improved mechanical and hardened martensite needle-like structure of metallurgical properties thereby saving the high cost of alloying.

KEYWORDS: Controlled Water Jet Impingement Cooling System, Impingement Gaps; Steel Plates, Mechanical & Metallurgical Properties

Received: Sep 14, 2021; **Accepted**: Oct 04, 2021; **Published**: Oct 22, 2021; **Paper Id.**: IJMPERDDEC202110

1. INTRODUCTION

Impingement is a process used to achieve a high yield of heat transfer extraction on materials for easy cooling**.** Impinging jets have been used to transfer heat in diverse applications, which include the drying of paper and textile materials, the cooling of turbine blades and in glass tempering works (Andrew and Hussain, 2013). They also noted that jet impingement cooling is also applied in electronics cooling, grinding process and inside vehicle wind-screen cooling, and in heat transfer, it is applied in cooling hot steel plates. Thus, steel companies that program to produce steel plates of various qualities and thicknesses invariably starts by re-heating the steel slabs obtained from the continuous –casting plant to rolling temperatures of about 900^{o}C (Hernandez, 2011).

To obtain normal microstructure and properties of good steels grades, water jet impingement cooling on the run-out table of a hot rolling mill is an important tool to realize the process. The improvement of advanced steel grades with adequate grained ferrite, pearlite and martensitic microstructures of good quality hardness has given

way for hot-rolled steel plates and strips (Carlestam, 2011). The cooling pattern and intensity employed in a hot mill of microstructural evolution have openly affected the process of austenite decomposition. In particular, finely grained microstructures are typically achieved through a controlled water jet impingement cooling system (Hatta *et al.*, 2010). It results in three boiling regimes, depending on the temperature of the steel surface (Tong and Tang, 2012). Heat is effectively removed when liquid water is directly in contact with the steel surface (nucleate and transition boiling), whereas it is substantially lower in the areas when the steel is covered by water vapor (film boiling) (Dhir, 2014; Wolf *et al.*, 2013).

Meanwhile, in order to study the thermal behavior of steel plates at low temperature range, the cooling process depends on a number of process parameters such as impingement gaps, H; pipe diameters, D; nozzle geometry water flow rate, Q; water temperature T_w; water pressure P_w; jet diameters D_{jet}; number of holes n; and speed of moving hot steel plates V. The effect of various parameters on the subsequent heat transfer rate on temperature-time cooling rates are investigated. To efficiently apply advanced cooling technologies for microstructure control, it is critical to develop suitable water jet impingement cooling system, evaluating its significant process parameters and determining an accurate zero-surface temperature model that predicts the temperature-time profiles during cooling of steel plates on run–out table system.

Therefore, the design and development of water jet impingement system is the panacea for induced desired mechanical and metallurgical properties in steel prior to its applications. Prodanovic (2004) at the University of British Columbia developed a more successful pilot plant of water jet impingement system for simulating industrial conditions of steel mills. Evaluation of the system showed promising results even though a constant impingement gap was adopted. However, this system in addition to some design shortcomings was not readily available locally for experimental analysis and this prompted the quest for a local alternative. Among the shortcomings were excessive tall structure that provided the required head of free water fall and fixed impingement gap thereby undermining the effect of variable impingement gap on the treated steel plates. Moreover, on the run-out tables in hot steel mills, the stationary or moving steel plates/strips typically cooled by water jets impinging on the surface of the hot steel was conveyed from the furnace through complicated and expensive hydraulic/chain drive system imposing serious challenge on providing a local but simple and efficient alternative. Consequent upon this an adequate hot plate conveying mechanism is desired.

This work, therefore, attempts to modify the design, construct and develop a controlled top water jet impingement cooling system that will influence the thermal behavior of steel plates at low temperature range by conducting systematic experimental studies on the pilot scale run-out table. The plant was constructed using locally sourced materials and installed in Metallurgical and Material Engineering Laboratory (MMEL) at ESUT, from the temperature range of 750^{o}C to 800^{o}C to initial temperature around 550^{o}C and controlled to 160 to 200^{o}C. Its performance was evaluated and compared with an existing foreign counterpart while the significant process parameters that influence the plate thermal responses were exhaustively determined. The mechanisms of conductive, convective and evaporative (boiling) heat transfers on a stationary plate were employed in the modeling mechanistic predictive model for the plate top zero-surface temperature (T_o). Characterization of heat flux during water jet impingement cooling formed the bases on which to carry out the system parametric studies. Thereafter, the comparative evaluations of the mechanical and metallurgical properties of the water jet impinged-cooled steel plates were conducted.

DESCRIPTION OF MATERIALS

The materials used in this study were locally sourced from Kenyeta Market Enugu, Onitsha Bridge Head Market, and

Idumota Market Lagos. There were two over-head water tanks, electric water pump of 0.373kw, 9kw electric heater, screw conveyor bed materials, workpiece of low carbon steel, workpiece carrier materials, ball gauge socket, flow meter, pressure gauge, PVC pipes, water reservoir, k-type thermocouple wires, 25mm shaft diameter of 1930mm long, control panel mounted on a stand, electric motor of 0.947kw, furnace support, stopwatch, electric furnace and water collector. For mechanical and metallurgical test analysis, the instruments used were: Optical Microscope Machine of 100µm at 100X magnification, Rockwell Test Machine of 10kg load and Charpy V-notch Impact machine load of 300 Joules, fixed and maximum heights of 1600mm and 1000mm.

Design Methodology and Analysis of Improved Water Jet Impingement System

The design methodology and analysis of the water jet impingement cooling system is based on: the design concepts and considerations; determination of power screw conveyor system; determination of critical speed of power screw conveyor system; determination of pressure head; instrumentations and thermocouples installation.

Design Concepts and Considerations

A locally constructed controlled water jet impingement cooling system was developed to simulate industrial cooling situations for run-out table cooling of plates in hot strip and plate as a modification of the Prodanovic *et al.*, (2004) model. The system allows heat transfer to be studied during cooling of hot steel plates of mill lines in industrial cooling. The following concepts and considerations brought about the modifications of the controlled water jet impingement cooling of hot-rolled steel plates in a Laboratory unit.

- Compactness and portability: Improvement was done in the existing rig by introduction of water pump for increased pressure head as against the free fall of the existing Prodanovic design thereby eliminating the excessive tall structure that provided the required head.
- Also, there was replacement of complicated and expensive hydraulic/chain conveyor mechanism of the existing rig with screw conveyor mechanism, for improved Water Jet Impingement Cooling System.
- Locally sourced materials of PVC pipes were used for the introduction of variable impingement gaps for replacement of fixed impingement gap to develop an improved Water Jet Impingement Cooling System for continuous cooling of hot-rolled steel plates.

The design considerations upon the modification were based on achieving good cooling rate through jet water impingement for improved mechanical and metallurgical properties of hot rolled steel plates. In addition, the adequate safety of operation is needed since the end result is to achieve good low-cost steel grades through safe but simplified processes which were before now achieved only by expensive alloying.

Determination of Power Screw Conveyor System

The powered screw conveyor bed carried an electric motor of 100 rpm and capacity of 1.27hp (0.947kw); a screw of M20×2.5mm, a bed frame made of angle iron (50.8mm x 50.8mm) and of mild steel plate of 4mm thickness. The angle iron was cut to specifications of 10 x 120 x 230 mm and the carriage of 231mm by 121 mm as shown in Appendix A. Other parts are the limiting switch and 3 k-typed thermocouples connected to a control panel.

The total power, P_T given by Equ. (1), required in the operation of conveyor system comprises power at a load P

of 2.2kg, power at maximum load P_1 and power consumed by the distribution of the $P_{2,\ P1}$ was determined as 251.71W from Equ. (2), P2 as 605W from Equ. (3) and P_2 as 353.3 W (assumed to be 58.4% of P_1).

$$P_T = P_1 + P_2 \quad (1)$$

$$P_1 = T_1 v \quad (2)$$

$$P_2 = W_T v \quad (3)$$

Therefore, the power requirement to derive this machine at maximum capacity and factor of safety of 1.5 was determined to be 0.947kw (1.27hp). Hence, an electric motor of 1.5hp was selected.

Determination of Critical Speed of Power Screw Conveyor System

The supporting bearing friction is assumed to be negligible. The bearings supporting the shaft are assumed accurately aligned with the shaft being linearly elastic. For the simply supported uniform load of 2.2kg of Figure 1, the length of the shaft is 1930mm, the diameter is 25mm, with the bearing support at both ends. One end of the shaft is fixed at the flexible coupling to an electric motor. The free body diagram for a uniform distributed load is shown in Figure 2.

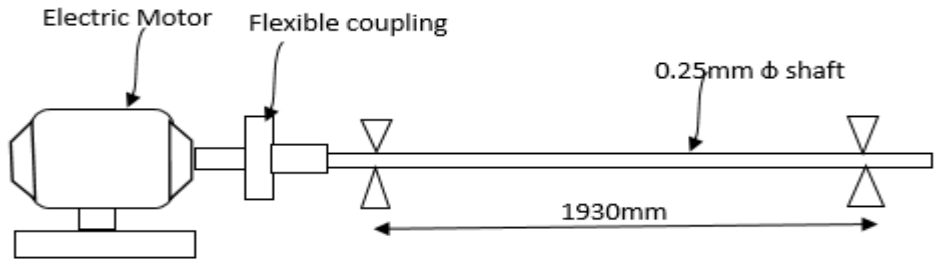

Figure 1: Shaft Support at Uniform Load.

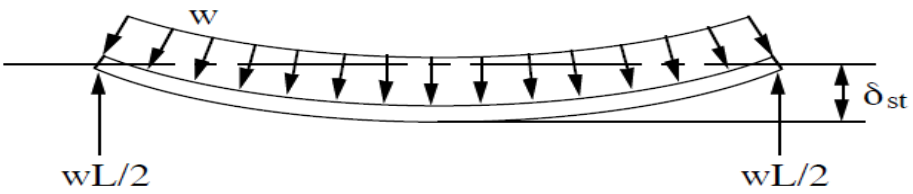

Figure 2: Free Body Diagram for Uniform Distributed Load.

The weight $0.0137kg/m$ of the free body diagram of Fig. 2 was determined using relation of Equ. 4 as,

$$w = A\rho = \frac{\pi d^2}{4} \quad (4)$$

Where ρ = 0.28kg/m^3 for steel; from the databook of (Khurmi and Gupta, 2005)

The stress strength (∂_{st}) of the shaft determined as$4.324x10^{-4}$, was gotten from the relation of Equ. (5), by (Khurmi and Gupta, 2005), as;

$$\partial_{st} = \frac{5wl^4}{384WI} \quad (5),$$

For a uniformed load distribution; E = 30x10^6 N/m^2 (Khurmi and Gupta, 2005)

Where $I = \frac{\pi d^4}{64}$ (6)

The critical speed (Π_c) of the shaft was determined as $199.73rpm$ using Equ. (7) given by Khurmi and Gupta, 2005), as;

$$\Pi_c = \sqrt{\frac{5g}{4\partial_{st}}} \quad (7)$$

Determination of Pressure Head

The impingement length of the pipe was measured to be 1900mm and the different discharge impingement gaps were 40mm, 50mm, 60mm, and 70mm respectively. The difference in height for each discharge was given as;

$$\begin{bmatrix} \Delta H_1 = 1900 - 40 = 1860 \\ \Delta H_2 = 1900 - 50 = 1850 \\ \Delta H_3 = 1900 - 60 = 1840 \\ \Delta H_4 = 1900 - 70 = 1830 \end{bmatrix} \quad (8);$$

From the experiment, minimum and maximum pressures are 2.8 2.8 N/m^2 and 3.1 2.8 N/m^2 respectively. The pressure head (H) at 2.8 N/m^2 and 3.1 2.8 N/m^2 were determined when ρ was at 50^{o}C as 29.03m and 32.14m using Equ. (9), as;

$$H = \frac{p}{\rho g} \quad (9)$$

Therefore, a centrifugal pump of head 32.14m and discharge of 7.14x10^{-5} m^3/s was selected to provide the equivalent head achievable in the existing design by elevation of the overhead tank for water free fall.

The flow rate and jet velocities were determined from equs. 10 and 12 as;

$$Q_{jet} = \frac{Q_{flow\ rate}}{30} \quad (10)$$

$$\mathrm{A} = \frac{\pi D^2}{4} = \frac{3.142_{\times} 0.0008^2}{4} = 5.027 \times 10 - 7m^2 \quad (11)$$

$$\text{Similarly, } v_{jet} = \frac{Q_{jet}}{A} = \frac{\frac{Q_{flow\ rate}}{30}}{\frac{\pi D^2}{4}} = \frac{4Q}{30\ x\ \pi\ x\ 0.0008^2} = \frac{4Q}{0.00006033}\frac{\mathrm{m}}{\mathrm{s}} \quad (12)$$

Manufacturing Procedure and Description of Water Jet Impingement Cooling System

The furnace comprises the internal and external casing. The internal casing was 49.49mm x 100mm with a depth of 84.04mm that served as support for the refractory box. It was rigidly fixed to accommodate the weight of the bricks, whereas the external casing of 460mm x 500mm was used for sides, 420mm x 450mm was used for the top and bottom plates and 420mm x 500mm was used for the back cover to house the entire furnace system, with the charging door. The charging door was 2mm mild steel flat sheet of 160mm x 172mm. A temperature controller that read 1200^{o}C was used since the maximum temperature of the heated workpiece in the furnace was 800^{o}C. The sheet metal meant for the fabrication of the furnace door was cut to 200mm x 420mm dimensions. A thermocouple of ± 50^{o}C was used. It has 6.62mm regulating filament with a head of 21.24mm and 24.29mm in diameter.

Two INTERDAB pressure gauges, calibrated in red from 0 to 10 bars with a measurement error of ±0.1 were mounted on the flow lines; one at the bend and the other before the flow meter. A SOCAM flow meter of model 510PR water-based fluids was used. It had 80mm diameter by 200mm height of 1000 digits' calibration with ± 1% accuracy and measured in m^3. An ATLAS water pump flow rate of 60L/min were used to circulate water throughout. It was ATP 60, 2850rpm speed and a voltage of 230 volts. It had a capacity 0.373kw and a current of 2.5 amp with a 50Hz frequency of single phase V.C of 45 and 10μf. The stopwatch was a Herwine type, calibrated from 0 to 60 seconds, with the inside calibration of 1 to 30 minutes. It had a ± 0.1-second accuracy error. The volumetric measuring cylinder calibrated from 50mm to 500mm was used to measure the volume of unevaporated water. Four diameters PVC pipes of 20mm, 25mm, 32mm, and 45mm, were used to carry four impingement gaps of 40mm, 50mm, 60mm, and 70mm. at ratio of 2: 2.5: 3.2: 4.5 to 4: 5 :6 : 7 respectively. The jet nozzles used had a cross section of 12 x 12mm of 30 number holes with 0.8mm jet diameter. It was made of brass material with a rounded nozzle exit. It was adjustable to allow for the range of experiments.

The thermocouple was tested by inserting the tip inside boiled hot water in a flask, with the other two ends connected to the digital control panel. The test recorded 97°C with an error of ± 3.0°C. K-typed thermocouple was used for temperature measurement because of its advantages, response time, its reliability and accuracy. It read a temperature up to 1260°C. Its wires contained two 0.254 mm diameter wires (Chromel and Alumel) that were insulated from each other by MgO powder and sheathed with stainless steel.

The plates were instrumented with three k-type thermocouples, installed from the bottom surface of the Test plate to 1mm of the top surface as shown in Figure 3.3. A screw thread hole was drilled through the test plate from the bottom side at a desired measurement point of 1mm before the top surface, with 8mm in diameter. At each point, the screw of the thermocouple was screwed to make it tight. The supporting accessories with the three thermocouples are shown in Figure 3.4 with the spacing of 62.5 mm each on a 230mm by 120mm workpiece.

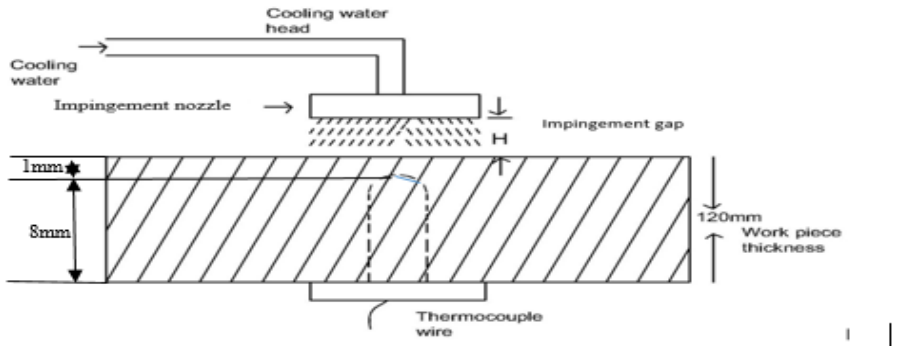

Figure 3: Sketch of Cooling Water and Thermocouple Installation.

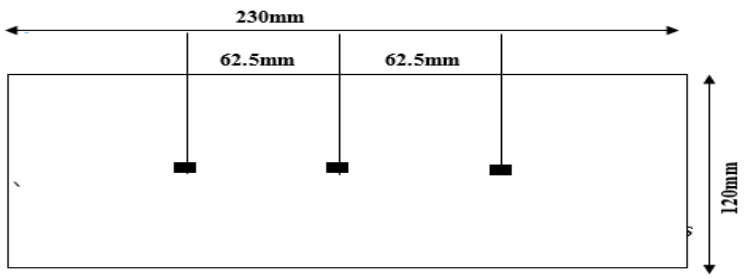

Figure 4: Sketch of Thermocouples Locations.

A pilot-scale run-out table (ROT) facility was designed, fabricated and installed in the Metallurgical and Material Engineering Laboratory (MMEL), ESUT. The schematic diagram of the pilot plant and photograph of the set-up are shown in Fig. 5 and Fig. 6 respectively. The detailed design drawings are presented in Appendix A. The heating was provided by an electric furnace where a steel plate was heated up to a temperature of 800^{o}C in Metallurgical and Material Laboratory ESUT Enugu. A motorized ASYNCHRONE ROTOR gear powered conveyor drive system of 750w of 1500rpm was used to operate a gear of 1:24 by the ratio with 50HZ. Under an AC. of 240volts, the steel plates were transported from the furnace to the cooling tower bed for the stationary experiments.

The cooling system featured a closed water loop where 0.945m^3 of water was circulated throughout the experiment through the cooling jet nozzles. Surface temperatures, water temperatures, impingement gaps and flow rates were controlled. An ATLAS (ATP 60) water pump that provided total water flow rates of 0.001m^3/sec was employed. It pumped water to the impingement plate from the water tank below through the flow meter, nozzle header via impingement jet nozzle to the hot plates. An electric heater of 9000w of 330volts was situated in the tank and was used to adjust the temperature of water between 10^{o}C to 70^{o}C. The water temperature readings were taken with mercury in bulb thermometer. A planar (water) nozzle with a cross-section of 12 x 12 mm size and 30 number holes of 0.8mm diameter was used. Also, a control panel mounted on a stand was used to read the initial and controlled cooling temperatures of the hot rolled steel plates.

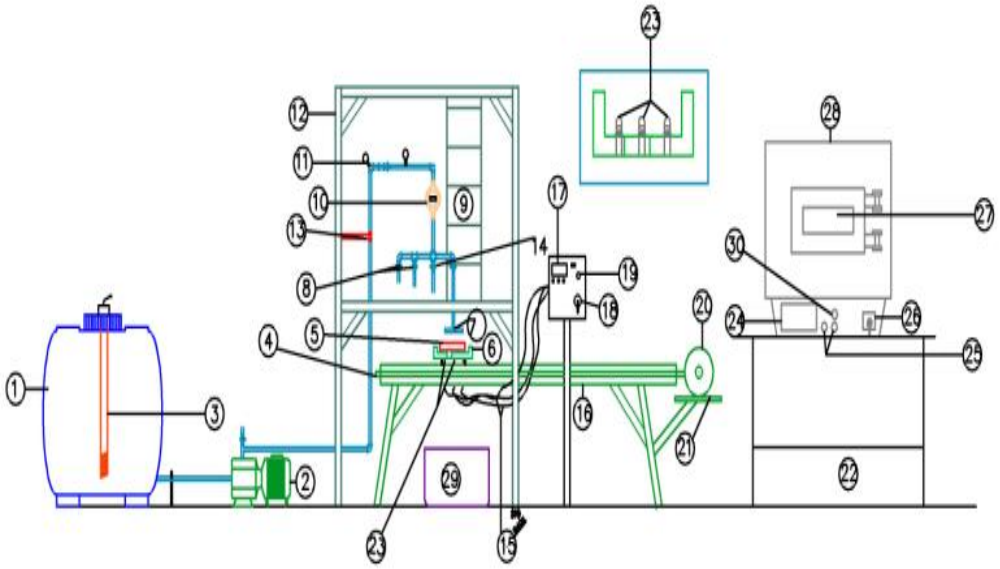

Figure 5: Schematic Diagram of the Pilot Plant.

1- Water tank, 2- Electric pump, 3-Heater, 4-Conveyor screw, 5-The workpiece, 6-Workpiece bed, 7-Impingement nozzle, 8-Ball gauge socket, 9-Ladder, 10-Flowmeter, 11-Pressure gauge, 12-Tower, 13-PVC pipe, 14-Reservoir, 15-Thermocouple wire, 16-Motorized Screw conveyor, 17-Thermocouple control panel, 18-The regulator, 19-Lock, 20-Electric motor, 21-Electric motor support, 2-Furnace support, 23-Thermocouple, 24-Furnace indicator, 25-Furnace switch, 26-Furnace regulator, 27-Furnace door, 28-Electric furnace, 29-Water collector, 30-Pilot light Header.

Figure 6: Photograph of the Developed Experimental Test Rig.

Performance Evaluation Procedure of Improved and Developed Water Jet Impingement Cooling System

The developed experimental rig (the pilot plant) was tested after fabrication and its performance was evaluated and compared with the existing rig. The test performance indicators include; the water flow rate, impingement velocity and gap, surface temperature, and cooling rate The work piece was heated to a temperature of 800^{o}C and transported towards the cooling jet area using the motorized screw conveyor. The center of the plate was positioned under the jet nozzle, and the water pump connected to the tank was turned on. The water header was positioned for different volume flow of water using different water pipe diameters and gaps. The pressure gauge and flow meter were also opened to read the values of pressure and volume flow rate was determined using the stopwatch. The initial surface temperatures of the plate (T_i) at the onset of water impingement cooling varied from 430 to 550^{o}C. Temperature data of various thermocouple locations were noted when the surface temperature was within +3^{o}C of the three thermocouples. The flow was timed at a controlled impingement cooling of 200^{o}C, 180^{o}C, 160^{o}C; 300^{o}C, 280^{o}C and 260^{o}C respectively. The evaporated water was obtained by subtracting the volume of water collected in the measuring cylinder from the volume of water recorded from the flow meter.

Experiments were carried out at several water flow rates. The water supply to the flow line through the flow meter to the hot plates through the header, and at various pipe diameters through jet nozzle was turned on at the pump. The 9000w electric heater was turned to vary the water temperatures. Thereafter, the readings of the process parameters of the impingement gaps, pipe flow diameters, initial temperatures of water between 30-70^{o}C, the final temperature of water, evaporated and un-evaporated water was read and recorded. Readings were monitored until nearly steady state isothermal condition was achieved i.e. T_1, T_2, T_3 were within 0.5% of each other with the average surface temperature of $\pm$3^{o}C. The final reading for the particular flow rate of water says, Q_1 of diameter, D, of 20mm with impingement gap, H, of 40mm were recorded. At that juncture, another three sets of experiments of pipe diameters of 25mm, 32mm, 45mm diameters and impingement gaps of 40mm, 60mm and 70mm each for different controlled temperature cooling of 160 to 200^{o}C and 260 to 300^{o}C were read and recorded. Subsequently, each flow of impingement water jet cooling, D, and H, were repeated as above. The pump provided variable head of 29 to 32m while the existing has a nearly constant head of 29m. The cooling rate of the existing rig operated at steady state planar jet type of 19mm jet diameter at fixed 150cm impingement gap with water temperature 30-95°C and 15-45 L/min using plate thickness 120mm plain carbon steel was compared with the

develop experimental rig using similar cooling conditions.

The plan for this study was based on the gaps created by (Hammad *et al.*, 2014), Monde and Inoue, (2013), Prodanovic and Wells, (2004) where impingement gaps, pipe diameters, water temperature, initial temperature and measurements positions were constants. Table 3.1 shows the experimental matrix variation with nozzle diameter (D mm), impingement gap (Hmm), volume of water used (Q_{US} m^3), volume of water unevaporated (Q_{Unevp} m^3), volume of water evaporated ($Q_{evp}m^3$), pressure (bar), time of cooling(s), flow rate (Q m^3/s), water temperature and initial temperature (T_i ^oC and T_f ^oC), and jet velocity (V_{jet} m/s).

Table 1: Experimental Plan for Recording Data

Ex No	D (mm)	H (m)	Qus (m^3)	Q_{unevap} (m^3)	Q_{evap} (m^3)	P (bar)	T_{sat} (^oC)	Q (m^3/s)	T_f	T_i (^oC)	V_{Jet} m/s
A	D20	H_{40-70}	$Q_{us}1$	$Q_{unevap}1$	$Q_{evap}1$	P_1	T_1	Q_1	T_f1	T_i1	Jet_1
B	D25	H_{40-70}	$Q_{us}2$	Q_{unevap} 2	Q_{evap} 2	P_2	T_2	Q_2	T_f2	T_i2	Jet_2
C	D32	H_{40-70}	$Q_{us}3$	Q_{unevap} 3	Q_{evap} 3	P_3	T_3	Q_3	T_f3	T_i3	Jet_3
D	D45	H_{40-70}	$Q_{us}4$	Q_{unevap} 4	Q_{evap} 4	P_4	T_4	$Q_\$$	T_f4	T_i4	Jet_4

COMPARATIVE ANALYSIS PROCEDURE

Chemical composition of Low Carbon Steel (LCS) was first established prior to the mechanical and metallurgical test. The microstructural test, hardness and impact test constitute the mechanical and metallurgical tests The tested sample was a low carbon steel and has a melting point of 1600^{o}C. The process employed for the chemical composition test was the electrode spark method, carried out with Electrode Spark Equipment method at Angstrom V-aso Spectrometer, Eastern Metal's Limited Asaba, Nigeria. The average chemical composition results are shown in Table. 2. The microstructural tests of the specimens were carried out with an optical microscope. Tests were done under the optical microscopic examination of 100µm at 100X magnification to show the microstructural phase of the LCS before and after impingement cooling

Table 2: Chemical Composition Test of LCS

Steel chemical composition	Fe	C	Si	Mn	S	P	Cr	Ni	Mo	Cu
Wt. %	98.48	0.25	0.095	0.40	0.032	0.010	0.053	0.051	0.016	0.103
Steel chemical composition	Al	V	Co	Sn	As	Nb	Pb	W	B	
Wt. %	0.008	0.011	0.011	0.0377	0.010	0.000	0.000	0.050	0.0001	

The hardness tests were carried out with a digital displayed Rockwell hardness tester. The depth of penetration of an indenter (diamond), under a large 10kg load, was used to determine the penetrations. The hardness of the workpieces before impingement cooling was determined. The test of the specimen before impingement cooling as presented in Table 3 together with the properties of standard ones. While the test of hardness properties is presented in chapter four.

Table 3: Mechanical Properties of the Medium Carbon Steel Compared with the Standards from AISI (Spotts 2008) and Azom, (2012)

Properties	Impact Strength (J)	RHN
Test Sample	97	38.9
*C1035	44.3	B68

Toughness is a measure of the amount of energy a material can absorb before fracturing. It becomes of engineering importance when the ability of a material to withstand an impact load without fracturing is considered. The Charpy V-notch (CVN) technique was used to measure the impact energy of the samples. V-notch was machined into a bar specimen with a square cross-section. The impact load used was 300 Joules with a fixed height (h_1) of 1600 mm and a maximum height (h_2) of 1000mm, which was lower than the fixed height

Results of Performance Analysis of Improved and Developed Water Jet Impingement System

The cooling conditions used in this analysis are similar to those employed in the previous study. Table 4 shows the performance test of the locally developed water jet impingement ROT rig at constant maximum pipe diameter of 45mm, jet diameter of 8mm and water temperature of 60-70ºC. The initial surface temperature of the test plates was measured with thermocouples while jet flow rates and the jet velocities were determined from Equations 10 and 12 respectively in page 43.

Table 4: Performance test of the developed Experimental Rig (Pilot scale ROT Plant)

S/N (Exp. Runs)	Plate Thickness (mm)	Flow Rate (m^3/sec)	Jet Impingement vel. (m/s)	Impingement Gap (mm)	Surface Temp (ºC)	Cooling Time (sec)	Cooling Rate (ºC/sec)
1	120	$1.64x10^{-5}$	1.0588	40	505	104	36.31
2	120	$1.36x10^{-5}$	0.8104	50	495	119	34.08
3	120	$1.33x10^{-5}$	0.6132	60	450	125	33.72
4	120	$1.154x10^{-5}$	0.4736	70	455	128	33.10

The results of the performance test (Table 4) shows that at constant pipe diameter of 45mm, reducing flow rates and jet impingement velocities, increasing impingement gaps and varying initial surface temperature of 120mm thick test plate, there is a steady decrease in cooling rate due to prolonged cooling time. This established trend is consistent with the previous works of Prodanovic *et al*., (2004) and Nobari (2014). The analysis of variance results of these data revealed that there is a significant improvement in the modified test rig as compared to the existing version.

Table 5: Comparative evaluation of Water Jet Impingement Cooling System

Table 5: Comparative evaluation of Water Jet Impingement Cooling System

S/N Exp. Runs	Plate thickness (mm)	Existing Pilot ROT Results				Developed Experimental Rig Results			
		Impingement Gap (mm)	Flow Rate (m^3/sec) $x10^{-4}$	Jet Impingement vel. (m/s)	Cooling rate (ºC/s)	Impingement Gap (mm)	Flow Rate (m^3/s) $x10^{-5}$	Jet Impingement vel. (m/s)	Cooling Rate (ºC/s)
1	120	1500	2.5	2.3	29.40	40	1.77	1.1777	36.31
2	120	1500	4.17	3.1	31.10	50	1.36	0.8670	35.08
3	120	1500	5.83	3.9	33.90	60	1.07	0.7072	33.72
4	120	1500	7.5	4.8	34.23	70	0.946	0.6272	33.10
Mean	**120**	**1500**	5.0	**3.52**	**32.15**	**55**	**2.346x10-5**	**0.8446**	**34.55**

Furthermore, for all the experimental runs at varying operating parameters, the cooling rate of the developed experimental rig showed a higher cooling rate and this was occasioned by variation in impingement gap which was constant in the existing (Prodanovic and Wells, 2004). This, therefore, resulted in an 8% increase in cooling rate revealing that impingement gap affects cooling pattern of the test plate, hence a great advantage over existing technologies and

suitable to be used as experimental rig and for further analysis. Although Monde and Inoue (2013) reported a higher cooling rate (2% increase), the ANOVA result showed no significant difference in the cooling rates compared to the huge advantage of forced water jet impingement with simple cheap conveying system of the modified rig.

Comparative Analysis Results of Improved Water Jet Impingement Cooling

The results of the LCS before and after improved water jet impingement cooling were examined at known chemical composition under microstructural test, hardness and impact test

Microstructural Test before Impingement Cooling

The microstructure Figure 7 shows the microstructural phase of the LCS before impingement cooling.

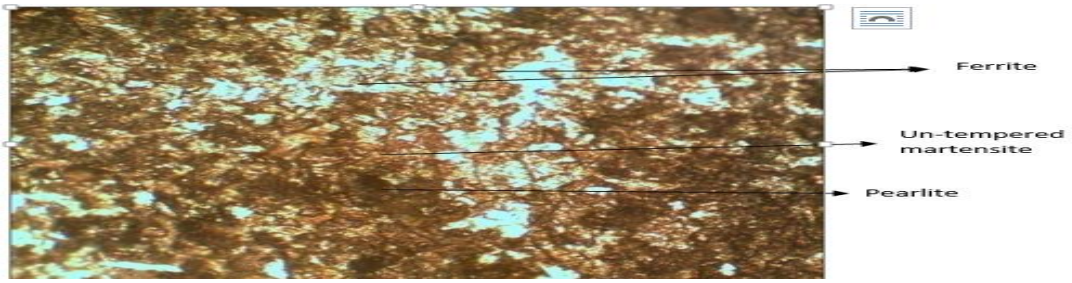

Figure 7: Sample of the Specimen before Impingement Cooling 100 x Magnifications.

The test showed an iron-carbon (98.480Fe - 0.25C) control sample of the optical micrograph of a mixed microstructure of bainite and pearlite in low carbon steel. The bainite was etched dark for the reason that it was a combination of ferrite and cementite. Contrarily the residual stage was un-tempered martensitic structure which etches lighter as a result of the lack of alloying advances. The presence of darker spot of pearlite indicates that the sample is a hypo eutectoid steel, between 0.008 to 0.76 wt%C (Callister, 2012).

Results of Microstructural Phase Transformation of the Micrographs after Impingement Cooling

The micrographs of Figures. 8, 9, 10 and 11, and Figs 12, 13, 14 and 15 respectively, showed the microstructural phase transformation from austenite temperature of 800^{o}C after water jet impingement cooling range of 438 to 500^{o}C, to a hardened needle-like martensitic form via ferrite and pearlite. The phase change of martensite occurred when the cooling rate from austenite was sufficiently fast in the different impingement gaps of 40mm and 70mm at different pipe diameters of 20mm, 25mm, 32mm, and 45mm. It was a hard constituent phase transformation due to the carbon which was trapped in the workpiece during impingement cooling. The temperature ranges of martensitic phase transformation occurred between 500^{o}C to below room temperature that depended on the hardenability of the specimen from the Rockwell Hardness test carried out as specified in literature. The martensite start temperature (M_s) to martensite finish temperature (M_f) is typical of the order of 150^{o}C to 300^{o}C (Savage, 2004); Ms = 500 to 300^{o}C- 35Mn – 20Cr and 15Ni.

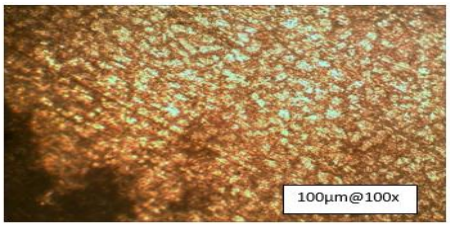

Figure 7: Sample of the Specimen before Impingement Cooling 100 x Magnifications

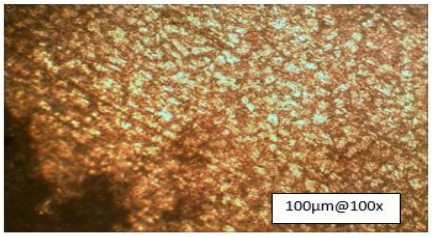

Figure 7: Sample of the specimen before Impingement Cooling 100 x magnifications

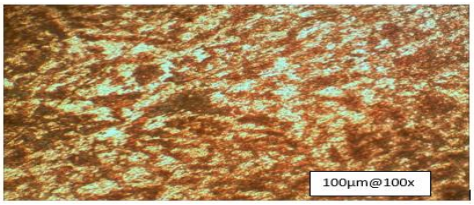

Figure 7: Sample of the specimen before Impingement Cooling 100 x magnifications

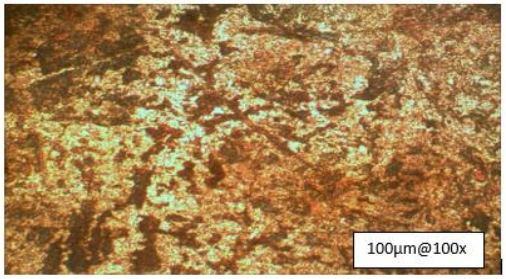

Figure7: Sample of the specimen before Impingement Cooling 100 x magnifications

Figures. 8, 9, 10 and 11 revealed the hardened martensitic phase transformed micrographs at constant pipe diameters of 20mm, 25mm, 32mm and 45mm at impingements gap of 70mm. The compositions at austenite temperature of 800°C have transformed through the dark ferrite and light pearlite to hardened scattered needles of martensitic structures. The phase transformations were achieved in figures, 9 and 10, but clearer martensitic structures were seen in figure11 where pipe diameter was 20mm at the high impingement gap of 70mm which bequeathed the product of good steel grades.

Similarly, Figures. 12, 13, 14 and 15 portrayed the hardened martensitic phase transformed micrographs at constant pipe diameters of 20mm, 25mm, 32mm and 45mm at impingements gap of 40mm.

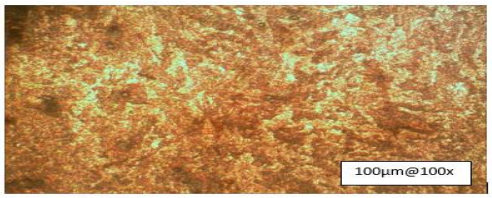

Fig. 12: D = 20mm & H- 40mm @ T_s = 500°C from 800°C of 109esc to 180°C

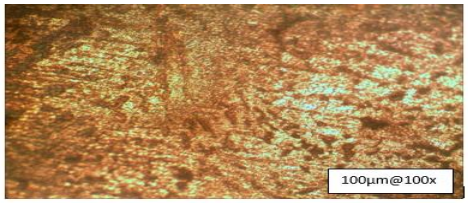

Fig. 13: D = 25mm & H- 40mm @ T_s = 500°C from 800°C of 110esc to 180°C

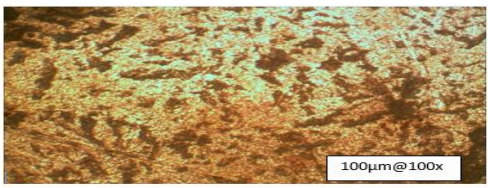

Fig. 14: D = 32mm & H- 40mm @ T_s = 470°C from 800°C of 112esc to 180°C

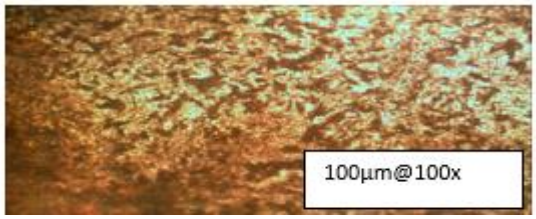

Fig. 15: D = 45mm & H- 40mm @ T_s = 458°C from 800°C of 102esc to 180°C

The compositions at austenite temperature of 800°C however, at this point had transformed through the dark ferrite and light pearlite to hardened scattered needles of martensitic structures. Also, the phase transformations were achieved in Figures. 13 and 14 but showed high martensitic structures at big pipe diameter of 45mm at impingement gap of 40mm Figure.15, which correspondingly gave the product of good (advanced) steel grades.

Results of Comparative Analysis of Hardness Test Results Before and after Improved Water Jet Impingement Cooled Steel Plate

The test results of the samples before and after water jet impingement cooling were shown in table 6. The Table showed RHT at the right, center and left with the compared result as control before impingement cooling.

Table 6: Rockwell Hardness Test Results of the Workpieces at 200oC

Rht Samples	Result before Impingement	Rhn Left Result after Impingement	Rhn Centre Result after Impingement	Rhn Right Result after Impingement
D=20mm,H= 40mm @ 200°C	38.9	46.4	53	46
D=20mm,H= 70mm @200°C	38.9	50.1	59.5	50.4
D=45mm,H=40mm @200°C	38.9	50.3	70	50
D=45mm,H= 70mm@200°C	38.9	44	55	44.3

The hardness comparative analysis of hardness test results for different pipe diameters of 20mm, 25mm, 32mm, and 45mm at impingement gaps of 70mm and 40mm were represented in Tables 7 and 8. The comparative results were shown in Figure 16.

Table 7: Rockwell Hardness Sample for Pipe Diameters of 20mm, 25mm, 32mm and 45mm at Constant Impingement Gap of 70mm.

Rht Samples	Result before Impingement	Rhn Left Result after Impingement	Rhn Centre result after Impingement	Rhn Right Result after Impingement
D=20mm,H= 70mm @200^{0}C	38.9	50.1	59.5	50.4
D=25mm,H= 70mm @ 200^{0}C	38.9	45.4	58.6	45
D=32mm,H= 70mm @200^{0}C	38.9	45	57.9	45
D=45mm,H= 70mm @200^{0}C	38.9	44	55	44.3

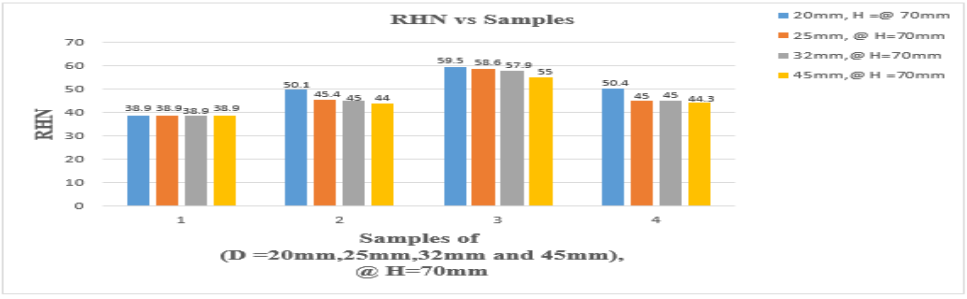

Figure 16: RHN Test Charts for Pipe Diameters of 20mm, 25mm,

Figure 16 illustrated that with 20mm pipe diameter at the impingement gap of 70mm, the hardness number was 59.5, followed by a 32mm diameter of hardness number 58.6. Then with diameter 25mm, the hardness was 57.9. However, the lowest hardness number 55 occurred at 20mm diameter. Moreover, the hardness decreased from smaller pipe diameter flow to bigger pipe diameter at the constant impingement gap of 70mm.

The microstrcture, Figures. 8, 9, 10 and 11, showed the grain transformation from austenite to martensitic phase. Figure 8 showed traces of martensite, and had the least hardness number of 55. Figures. 9 and 10, showed dark hardened martensitic formations from ferrite and pearlite with hardness numbers 57.9 and 58.6 of Figure 16. However, figure 11 showed fine clearer hardened transformed martensite, from austenite 800^{o}C for 1hr, exposed to the surface temperature of 438^{o}C at smaller pipe diameter and higher impingement gap. Then, cooled to 180^{o}C through ferrite and pearlite phases with the highest hardness number of 59.5 by 53%, which suggested good advanced steel grades as specified by (Azom, 2012 and Microalloy, 2005).

Table 8: Rockwell Hardness Sample for Pipe Diameters of 20mm, 25mm, 32mm and 45mm at Constant Impingement Gap of 40mm

Rht Samples	Result before Impingement	Rhn Left Result after Impingement	Rhn Centre Result after Impingement	Rhn Right Result after Impingement
D=20mm,H= 40mm @ 200^{o}C	38.9	46.4	53	46
D=25mm,H= 40mm @ 200^{o}C	38.9	48	54.1	47.8
D=32mm,H= 40mm @ 200^{o}C	38.9	49.8	62.1	50
D=45mm,H= 40mm @ 200^{o}C	38.9	50.3	70	50

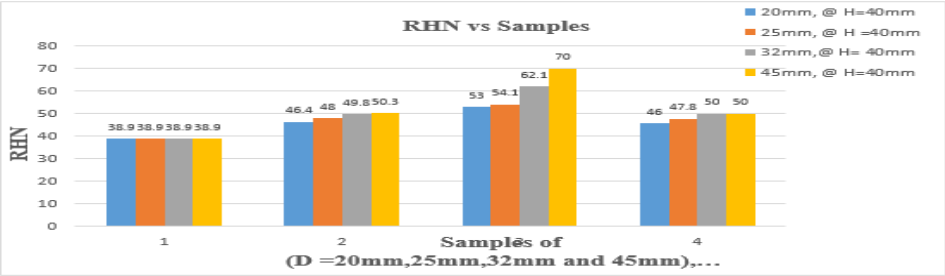

Figure 17: RHN Test Charts for Pipe Diameters of 20mm, 25mm, 32mm and 45mm at Impingement Gap 40mm.

The microstrcture Figures. 12, 13, 14 and 15, showed that the grain transformed from austenite to the martensitic phase. Fig. 12, showed traces of martensite and had the least hardness number of 53. Figures 13 and 15, showed dark hardened martensitic formations from ferrite and pearlite with hardness numbers 54.1 and 62.1 of Figure17. However, figure15 showed fine clearer hardened transformed martensite from austenite temperature of 800^{o}C for 1hr, exposed to the initial temperature of 470^{o}C at bigger pipe diameter and smaller impingement gap. Then, cooled at 180^{o}C through ferrite and pearlite phases with the highest hardness number of 70. This equally suggested good advanced steel grades as specified by (Azom, 2012 and Microalloy, 2005).

Results Comparative Analysis of Impact Test Results Before and after Improved Water Jet Impingement Cooled Steel Plate

Based on the difference between h and 'h', the energy absorption of the specimens was read and recorded as shown in Tables 9 and 10.

Table 9: Charpy V-Notch Sample Test for Pipe Diameters of 20mm, 25mm, 32mm and 45mm at constant Impingement Gap of 40mm

CVN Test Sample (Joules)	Control CVN Sample Test (Js)	left CVN(Js)	Center CVN(Js)	Right CVN(Js)
D=20mm,H= 40mm @ 200^{0}C	97	79	61	81.5
D=25mm,H= 40mm @ 200^{0}C	97	76	59	77
D=32mm,H= 40mm @ 200^{0}C	97	71	58	73
D=45mm,H= 40mm @ 200^{0}C	97	69	56	70

Table 10: Charpy V-notch Sample Test for Pipe Diameters of 20mm, 25mm, 32mm and 45mm at Constant Impingement Gap of 70mm

CVN Test Sample (Joules)	Control CVN sample test (Js)	left CVN(Js)	Center CVN(Js)	Right CVN(Js)
D=20mm,H= 70mm @ 200^{0}C	97	80	63	83
D=25mm,H= 70mm @ 200^{0}C	97	77.5	61	78
D=32mm,H= 70mm @ 200^{0}C	97	73	59	74.5
D=45mm,H= 70mm @ 200^{0}C	97	71	57	72

The impact tests of Tables 9 and 10 were shown in Figures. 18 and 19. The graphs showed that the effect of impact energy was lower at the center and higher at both ends. However, 18 showed that impact energy of the control samples was higher than the impinged samples.

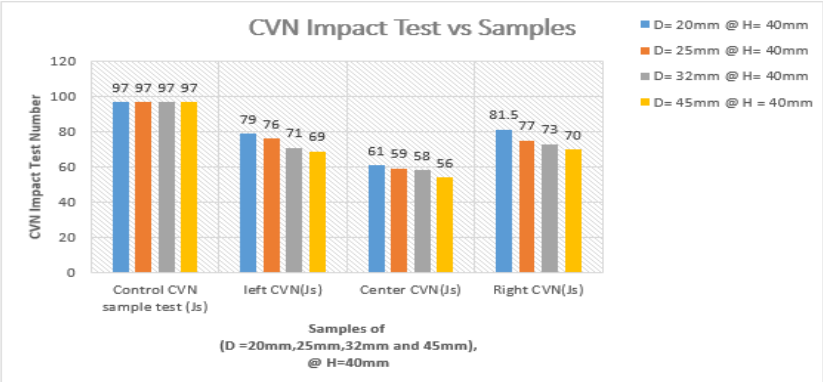

Figure 18: Impact Test Charts for Pipe Diameters of 20mm, 25mm, 32mm and 45mm at Impingement Gap 40mm.

Figure 18 showed that with pipe diameter 20mm at the impingement gap 40mm, the impact energy was 61Js, followed by pipe diameter 25mm of impact energy 59 Js. Then with pipe diameter of 32mm, the impact energy was 58 Js. The lowest impact energy 56 occurred at pipe diameter of 45mm. Meanwhile, it showed nearly the same energy at the other ends. This is a result of convectional cooling from the impingement target. However, impact energy increased from 56J of pipe diameter 45mm to 61J pipe diameter 20mm at impingement gap of 40mm of 26.4% to 37.7% as against 44.3J,

specified by AISI, (Spotts 2008) and Azom, (2012).

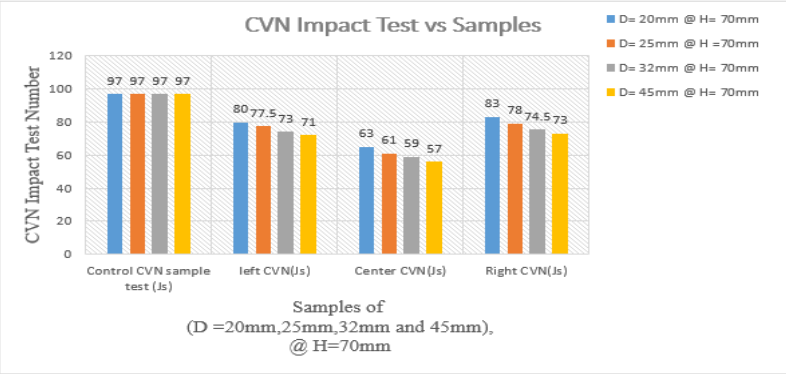

Figure 19: Impact Test Charts for Pipe Diameters of 20mm, 25mm, 32mm and 45mm at Impingement Gap 70mm.

Figure 18 showed that with pipe diameter 20mm at impingement gap 70mm, the impact energy was 63Js, followed by 25mm pipe diameter of impact energy 61 Js. Then with a pipe diameter of 32mm, the impact energy was 59 Js. However, the lowest impact energy 57 occurred at a pipe diameter of 45mm. It also showed that the impact energy was also recorded lowest at the impingement target and showed nearly the same energy at the other ends, equally as a result of convectional cooling from the impingement target. Also, the impact energy correspondingly increased from 57J of pipe diameter 45mm to 63J pipe diameter of 20mm at impingement gap of 70mm by 28.67% to 42.2% as against 44.3J, specified by AISI (Spotts 2008) and Azom, (2012).

CONCLUSIONS

Comparative performance results revealed an 8% increase in the cooling rate of the improved system over the existing technology. Results further showed that with a tested-plate initial temperature at 550^{o}C, a controlled cooling temperature of 160^{o}C was achieved which produced film and nucleate boiling heat extraction effect. This influenced microstructural properties of the test plates. The plates post treatment examinations of the grain microstructure and mechanical properties revealed good martensite-phase transformation and enhanced "advanced-steel" hardness of Rockwell 59.9 respectively. In addition, the impact energy test showed a good value range of 56 to 63J which compares favorably with the AISI standard of 44.3J. This, therefore, gave 53% hardness and 26% to 42.2% impact of improved mechanical and hardened martensite needle-like structure of metallurgical properties thereby saving the high cost of alloying.

ACKNOWLEDGEMENTS

The authors are grateful to Enugu State University of Science and Technology for providing space and Laboratory for this research work

REFERENCES

1. *Andrew, G.E., and Hussain, C.I. (2013). Impingement Cooling of Gas Turbine Components. Tokyo International Gas Turbine Congress, Paper 83-Tokoyo-IGTC-9.*
2. *Azon (2012). Mechanical Properties of Low Carbon Steel of AISI. 1018.www.azonco/article.aspex?*
3. *Callister, W.O., D. Jr. and Thomas, B.G. (2008). "Phase Transformation of formation from Austenite".(7th Ed).*

4. *Callister, William, D. Jr. (2012). Materials Science and Engineering, an Introduction (7th Ed.), Part 001.*
5. *Carlestam, A., (2011). Effect of Microstructural on Hot Steel Plates. International Symposium on the Recent Developments in Plate, Vol.5 p200-207 Steels.*
6. *Dhir, V.K. (2014). "Boling heat transfer", Annual Review of Fluid Mechanics,30: 365- 401.*
7. *Hammed, J., Mitsutake, Y., Monde, M. (2014). International Journal of Heat and Mass Transfer, 43: 743 – 757.*
8. *Hatta, N., Tanaka, Y., Takuda, H., and Kakado, J.-I. (2010). A numerical study on cooling of hot steel plate by a water curtain. Trans. ISIJ, 29:673– 679, 1989.*
9. *Hernandez, V.H. (2011). Modelling of Thermal Evolution on Steel Strips cooled in the rolling Run-out Table, Ph.D Thesis, MMAT, University of British Columbia.*
10. *Khurmi and R.S. Sedha(2012). Theory of metal on Carbon Steels and Mechanical Properties of Medium Carbon Steel.*
11. *Monde, M., Inoue, T., (2013). Journal of Heat Transfer, 113: 722-727.*
12. *Prodanovic, V., Fraser, D., and Mihtzer, M. (2004). Simulation of Run-out Table Cooling by Water Jet Impingement on Stationary Plates – A novel experimental Method, 2nd International Conference on Thermochemical processing of Steel Ed. M. Lamberights, Liege, Belgium, 25-320.*
13. *Tong, L.S., and Tang, Y.S. (2012). Boiling Heat Transfer and Two-phase Flow, 2nd ed., Taylor and Francis, Washington, D.C:1-10.*
14. *Wolf, D. H., Incropera, F. P., Viskanta, R. (2013). Advances in Heat Transfer, 23:1-131.*
15. *Kumar, S. Narasimha. "Comparative Study of Performance, Combustion and Exhaust Emissions Analysis of Linseed Oil Based Biodiesel in a Ceramic Coated Diesel Engine." International Journal of Mechanical and Production Engineering Research and Development (IJMPERD) 4.2 (2014): 75-98.*
16. *Janardhan, N., et al. "Control of exhaust emissions of jatropha oil in crude form and biodiesel from high grade low heat rejection diesel engine." International Journal of Mechanical and Production Engineering Research and Development 3.2 (2013): 199-212.*
17. *Rao, N. Venkateswara, MVS Murali Krishna, and P. V. K. Murthy. "Comparative Studies on Performance Parameters of Tobacco Seed Oil in Crude form and Biodiesel form in Direct Injection Diesel Engine." Research and Development (IJAuERD) 3.4 (2013): 57-72.*
18. *Ghosh, S., and SK Saha. "An Experimental Leak Test Facility for Subcooled Water Leakages." International Journal of Mechanical and Production Engineering Research and Development (IJMPERD) 4.5, Oct 2014, 1-12*